Constant Power Control of Dfig Wind Turbines With Supercapacitor Energy Storage

A.Ramana[1], D.Chinnakullay reddy[2]
M.Tech, Madanapalle Institute of Technology & Science
M.Tech; Asst.Professor, Madanapalle Institute of Technology & Science

Abstract—With the increasing penetration of wind power into electric power grids, energy storage devices will be required to dynamically match the intermittency of wind energy. This paper proposes a novel two-layer constant power control scheme for a wind farm equipped with doubly fed induction generator (DFIG) wind turbines. Each DFIG wind turbine is equipped with a super capacitor energy storage system (ESS) and is controlled by the low-layer wind turbine generator (WTG) controllers and coordinated by a high-layer wind farm supervisory controller (WFSC). The WFSC generates the active power references for the low-layer WTG controllers according to the active power demand from or generation commitment to the grid operator; the low-layer WTG controllers then regulate each DFIG wind turbine to generate the desired amount of active power, where the deviations between the available wind energy input and desired active power output are compensated by the ESS. Simulation studies are carried out in PSCAD/EMTDC on a wind farm equipped with 15 DFIG wind turbines to verify the effectiveness of the proposed control scheme.

Index Terms—Constant power control (CPC), doubly fed induction generator (DFIG), energy storage, supervisory controller, wind turbine.

I. WIND TURBINE

Generators (WTGs) are usually controlled to generate maximum electrical power from wind under normal wind conditions. However, because of the variations of the wind speed, the generated electrical power of a WTG is usually fluctuated. Currently, wind energy only provides about 1%–2% of the U.S.'s electricity supply. At such a penetration level, it is not necessary to require WTGs to participate in automatic generation control, unit commitment, or frequency regulation. However, it is reasonable to expect that wind power will be capable of becoming a major contributor to the nation's and world's electricity supply over the next three decades. For instance, the European Wind Energy Association has set a target to satisfy more than 22% of European electricity demand with wind power by 2030 [1]. In the U.S., according to a report [2] by the Department of Energy, it is feasible to supply 20% of the nation's electricity from wind by 2030. At such high levels of penetration, it will become necessary to require WTGs to supply a desired amount of active power to participate in automatic generation control or frequency regulation of the grid [3]. However, the intermittency of wind resources can cause high rates of change (ramps) in power generation [4], which is a critical issue for balancing power systems. Moreover, to optimize the economic performance of power systems with high penetrations of wind power, it would be desired to require WTGs to participate in unit commitment, economic dispatch, or electricity market operation [5]. In practice, short-term wind power prediction [6] is carried out to help WTGs provide these functions. However, even using the state-of-the-art methods, prediction errors are present [5]. Under these conditions, the replacement power is supported by reserves, which, however, can be more expensive than base electricity prices [7]. To enable WTGs to effectively participate in frequency and active power regulation, unit commitment, economic dispatch, and electricity market operation, energy storage devices will be required to dynamically match the intermittency of wind energy. In [8], the authors investigated and compared different feasible electric energy storage technologies for intermittent renewable energy generation, such as wind power. Currently, pumped water and compressed air are the most commonly used energy storage technologies for power grids due to their low capital costs [9]. However, these two technologies are mheavily dependent on geographical location with relatively low round-trip efficiency. Compared with their peers, batteries and supercapacitors are more efficient, have a quicker response to demand variations, and are easy to develop and ubiquitously deployable. Compared to batteries, supercapacitors have a higher power density, higher round-trip efficiency, longer cycle life, and lower capital cost per cycle [10]. Therefore, supercapacitors are a good candidate for short-term (i.e., seconds to minutes) energy storage that enables WTGs to provide the function of frequency regulation and effectively participate in unit commitment and electricity market operation. The use of supercapacitors [10] or batteries [11]–[13] as energy storage devices for WTGs has been studied by some researchers. However, these studies only focused on control and operation of individual WTGs and did not investigate the issues of WTGs to participate in grid regulation. This paper proposes a novel two-layer constant power control (CPC) scheme for a wind farm equipped with doubly fed induction generator (DFIG) wind turbines [14], where each WTG is equipped with a supercapacitor energy storage system (ESS).
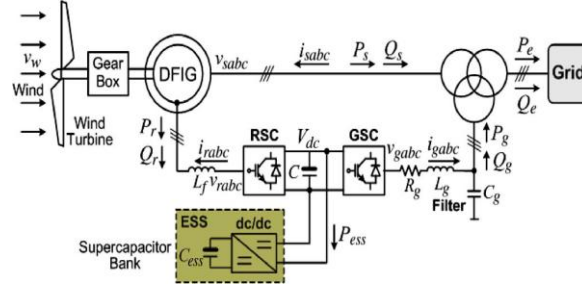
Fig. 1. Configuration of a DFIG wind turbine equipped
with a supercapacitor ESS connected to a power grid.

The CPC consists of a high-layer wind farm supervisory controller (WFSC) and low-layer WTG controllers. The highlayer WFSC generates the active power references for the lowlayer WTG controllers of each DFIG wind turbine according to the active power demand from the grid operator. The low-layer WTG controllers then regulate each DFIG wind turbine to generate the desired amount of active power, where the deviations between the available wind energy input and desired active power output are compensated by the ESS. Simulation studies are carried out in PSCAD/EMTDC for a wind farm equipped with 15 DFIG wind turbines to verify the effectiveness of the proposed control scheme.

II. DFIG WIND TURBINE WITH ENERGY STORAGE

Fig. 1 shows the basic configuration of a DFIG wind turbine equipped with a super capacitor-based ESS. The low-speed wind turbine drives a high-speed DFIG through a gearbox. The DFIG is a wound-rotor induction machine. It is connected to the power grid at both stator and rotor terminals. The stator is directly connected to the grid, while the rotor is fed through a variable-frequency converter, which consists of a rotor-side converter (RSC) and a grid-side converter (GSC) connected back to back through a dc link and usually has a rating of a fraction (25%−30%) of the DFIG nominal power. As a consequence, the WTG can operate with the rotational speed in a range of ±25%−30% around the synchronous speed, and its active and reactive powers can be controlled independently. In this paper, an ESS consisting of a super capacitor bank and a two-quadrant dc/dc converter is connected to the dc link of the DFIG converters. The ESS serves as either a source or a sink of active power and therefore contributes to control the generated active power of the WTG. The value of the supercapacitor bank can be determined by

$$C_{ess}=2P_nT/V_{SC}^2 \qquad (1)$$

where Cess is in farads, Pn is the rated power of the DFIG in watts, VSC is the rated voltage of the supercapacitor bank in volts, and T is the desired time period in seconds that the ESS can supply/store energy at the rated power (Pn) of the DFIG. The use of an ESS in each WTG rather than a large single central ESS for the entire wind farm is based on two reasons. First, this arrangement has a high reliability because the failure of a single ESS unit does not affect the ESS units in other WTGs. Second, the use of an ESS in each WTG can reinforce the dc bus of the DFIG converters during transients, there by enhancing the low-voltage ride through capability of the WTG [10].
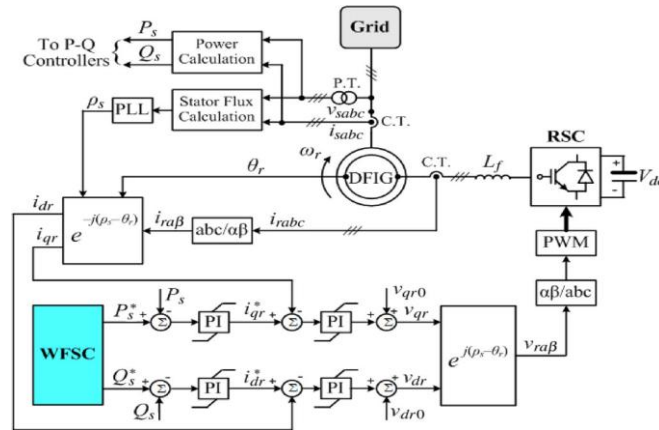

Fig. 2. Overall vector control scheme of the RSC.

III. CONTROL OF INDIVIDUAL DFIG WIND TURBINE

The control system of each individual DFIG wind turbine generally consists of two parts: 1) the electrical control of the DFIG and 2) the mechanical control of the wind turbine blade pitch angle [14], [15] and yaw system. Control of the DFIG is achieved by controlling the RSC, the GSC, and the ESS (see Fig. 1). The control objective of the RSC is to regulate the stator-side active power Ps and reactive power Qs independently. The control objective of the GSC is to maintain the dc-link voltage Vdc constant and to regulate the reactive power Qg that the GSC exchanges with the grid. The control objective of the ESS is to regulate the active power Pg that the GSC exchanges with the grid. In this paper, the mechanical control of the wind turbine blade pitch angle is similar to that in [15].

A.   Control of the RSC

Fig. 2 shows the overall vector control scheme of the RSC, in which the independent control of the stator active power P_s and reactive power Q_s is achieved by means of rotor current regulation in a stator-flux-oriented synchronously rotating reference frame [16]. Therefore, the overall RSC control scheme consists of two cascaded control loops. The outer control loop regulates the stator active and reactive power independently,which generates the reference signals $i*$ dr and $i*$ qr of the d- and q-axis current components, respectively, for the inner-loop current regulation. The outputs of the two current controllers are compensated by the corresponding cross-coupling terms $vdr0$ and $vqr0$ [14], respectively, to form the total voltage signals vdr and vqr. They are then used by the pulse width modulation (PWM) module to generate the gate control signals to drive the RSC. The reference signals of the outer-loop power controllers are generated by the high-layer WFSC.
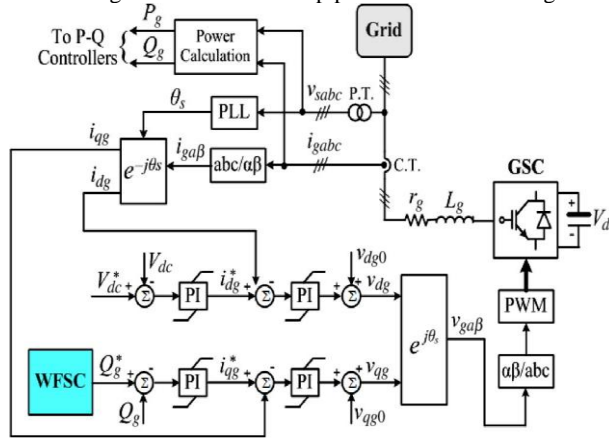

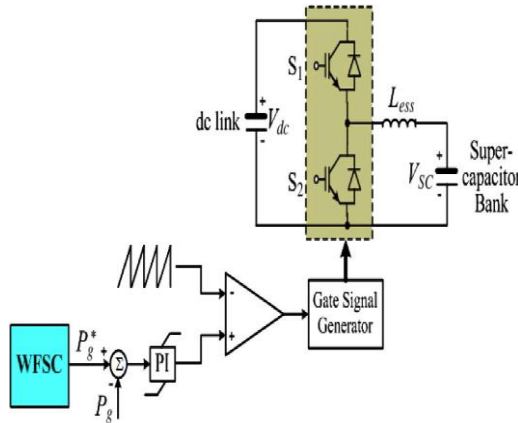*Fig. 3. Overall vector control scheme of the GSC.*

Fig. 4. Configuration and control of the ESS.

B. Control of the GSC

Fig. 3 shows the overall vector control scheme of the GSC, in which the control of the dc-link voltage Vdc and the reactive power Q_g exchanged between the GSC and the grid is achieved by means of current regulation in a synchronously rotating reference frame [16]. Again, the overall GSC control scheme consists of two cascaded control loops. The outer control loop regulates the dc-link voltage Vdc and the reactive power Q_g, respectively, which generates the reference signals $i*$ dg and $i*$ qg of the d- and q-axis current components, respectively, for the inner-loop current regulation. The outputs of the two current controllers are compensated by the corresponding cross coupling terms $vdg0$ and $vqg0$ [14], respectively, to form the total voltage signals vdg and vqg. They are then used by the PWM module to generate the gate control signals to drive the GSC.

The reference signal of the outer-loop reactive power controller is generated by the high-layer WFSC.

C. Configuration and Control of the ESS

Fig. 4 shows the configuration and control of the ESS. The ESS consists of a supercapacitor bank and a two-quadrant dc/dc converter connected to the dc link of the DFIG. The dc/dc converter contains two insulated-gate bipolar transistor (IGBT) switches S1 and S2. Their duty ratios are controlled to regulate the active power P_g that the GSC exchanges with the grid. In this configuration, the dc/dc converter can operate in two different modes, i.e., buck or boost mode, depending on the status of the two IGBT switches. If S1 is open, the dc/dc converter operates in the boost mode; if S2 is open, the dc/dc converter operates in the buck mode. The duty ratio $D1$ of S1 in

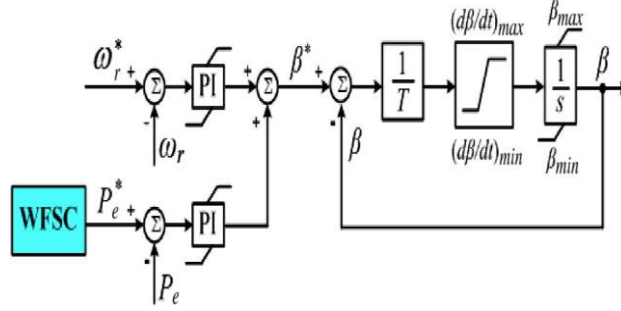the buck mode can be approximately expressed as D1=VSC/Vdc   (2)

Fig. 5. Blade pitch control for the wind turbine.

The operating modes and duty ratios $D1$ and $D2$ of the dc/dc converter are controlled depending on the relationship between the active powers Pr of the RSC and Pg of the GSC. If Pr is greater than Pg, the converter is in buck mode and $D1$ is controlled, such that the supercapacitor bank serves as a sink to absorb active power, which results in the increase of its voltage VSC. On the contrary, if Pg is greater than Pr, the converter is in boost mode and $D2$ is controlled, such that the supercapacitor bank serves as a source to supply active power, which results in the decrease of its voltage VSC. Therefore, by controlling the operating modes and duty ratios of the dc/dc converter, the ESS serves as either a source or a sink of active power to control the generated active power of the WTG. In Fig. 4, the reference signal $P*g$ is generated by the high-layer WFSC.

D. Wind Turbine Blade Pitch Control

Fig. 5 shows the blade pitch control for the wind turbine, where ωr and Pe ($= Ps + Pg$) are the rotating speed and output active power of the DFIG, respectively. When the wind speed is below the rated value and the WTG is required to generate the maximum power, ωr and Pe are set at their reference values, and the blade pitch control is deactivated. When the wind speed is below the rated value, but the WTG is required to generate a constant power less than the maximum power, the active power controller may be activated, where the reference signal $P*e$ is generated by the high-layer WFSC and Pe takes the actual measured value. The active power controller adjusts the blade pitch angle to reduce the mechanical power that the turbine extracts from wind. This reduces the imbalance between the turbine mechanical power and the DFIG output active power, thereby reducing the mechanical stress in the WTG and stabilizing the WTG system. Finally, when the wind speed increases above the rated value, both ωr and Pe take the actual measured values, and both the speed and active power controllers are activated to adjust the blade pitch angle.

IV.   WIND FARM SUPERVISORY CONTROL

The objective of the WFSC is to generate the reference signals for the outer-loop power controllers of the RSC and GSC, the controller of the dc/dc converter, and the blade pitch controller of each WTG, according to the power demand from or the generation commitment to the grid operator. The implementation of the WFSC is described by the flowchart in Fig. 6, where Pd is the active power demand from or the generation commitment to the grid operator; vwi and $Vessi$ are the wind speed in meters per second and the voltage of the supercapacitor bank measured from WTG i ($i = 1, . . . , N$), respectively; and N is the number of WTGs in the wind farm. Based on vwi, the optimal rotational speed $\omega ti,$opt in radians per second of the wind turbine can be determined, which is proportional to the wind speed vwi at a certain pitch angle βi

$\omega ti, opt = k(\beta i)vwi$ (3)

where k is a constant at a certain value of βi. Then, the maximum mechanical power $Pmi,$max that the wind turbine extracts from the wind can be calculated by the well-known wind turbine aerodynamic characteristics

$Pmi,\textbf{max} = 1/2\rho iArv3wiCPi(\lambda i,\textbf{opt}, \beta i)$ (4)

where ρi is the air density in kilograms per cubic meter; $Ar = \pi R2$ is the area in square meters swept by the rotor blades, with R being the blade length in meters; and CPi is the power coefficient, which is a function of both tip-speed ratio λi and the blade pitch angle βi, where λi is defined by

$\lambda i = \omega tiR/vwi.$ (5)

In (4), $\lambda i,$opt is the optimal tip-speed ratio when the wind turbine rotates with the optimal speed $\omega ti,$opt at the wind speed vwi.

Given $Pmi,$max, the maximum active power $Pei,$max generated by the WTG can be estimated by taking into account the power losses of the WTG [14]

$Pei,\textbf{max} = Pmi,\textbf{max} − PLi = Psi,\textbf{max} + Pri,\textbf{max}$ (6)

where PLi is the total power losses of WTG i, which can be estimated by the method in [14]; $Psi,$max and $Pri,$max are the maximum DFIG stator and rotor active powers of WTG i, respectively. In terms of the instantaneous variables in Fig. 1, the stator active power Ps can be written in a synchronously rotating dq reference frame [16] as follows:

$Ps = 3/2(vdsids + vqsiqs)$

$\approx 3/2[\omega sLm(iqsidr − idsiqr) + rs(i^2ds + I^2qs)]$ (7)

where vds and vqs are the d- and q-axis voltage components of the stator windings, respectively; ids and iqs are the stator d- and q-axis current components, respectively; idr and iqr are the rotor d- and q-axis current components, respectively; ωs is the rotational speed of the synchronous reference frame; and rs and Lm are the stator resistance and mutual inductance, respectively. Similarly, the rotor active power is calculated by

Pr =3/2(vdridr + vqriqr)
 ≈ *3/2[sωsLm(iqsidr − idsiqr) + rr[I ^{2}dr + I ^{2}qr](8)*
where *vdr* and *vqr* are the *d-* and *q*-axis voltage components of the rotor windings, respectively; *s* is the slip of the DFIG defined by
s = (ωs − ωr)/ωs   **(9)**
where *ωr* is the DFIG rotor speed. (7) and (8) yield
s = −(Pr − 3i^2 rr)(/Ps − 3i ^{2}srs)   **(10)**
where is =(I ^{2}ds + I ^{2}qs/2)$^{1/2}$ and
ir =(I ^{2}dr + I ^{2}qr/2)$^{1/2}$.
 If neglecting the stator copper loss 3i ^{2}s rs and rotor copper loss 3i ^{2}r rr of the DFIG, the relationship between the stator and rotor active powers can be approximated by *Pr = -sPs.* (11)

According to (6) and (10) [or (11)], *Psi,*max and *Pri,*max of each WTG can be determined. Then, the total maximum mechanical power *Pm,*max, DFIG output active power *Pe,*max, and stator active power *Ps,*max of all WTGs in the wind farm can be calculated as

$$P_{m,\max} = \sum_{i=1}^{N} P_{mi,\max} \qquad (12)$$

$$P_{e,\max} = \sum_{i=1}^{N} P_{ei,\max} \qquad (13)$$

$$P_{s,\max} = \sum_{i=1}^{N} P_{si,\max}. \qquad (14)$$

In order to supply constant power *Pd* to the grid, the deviation *Pess,d* between the demand/commitment *Pd* and the maximum generation *Pe,*max is the power that should be stored in or supplied from the ESSs of the WTGs *Pess,d = Pe,*max − *Pd.*

On the other hand, the capability of each ESS to store or supply power depends on the capacitance *C*ess and the voltage *Vessi* of the supercapacitor bank. During normal operation, *Vessi* must be maintained within the following range: **Vi,min < Vessi < Vi,max**   **(16)**

where *Vi,*max and *Vi,*min are the maximum and minimum operating voltages of the supercapacitor bank, respectively. The maximum power *Pessi,*max that can be exchanged between the supercapacitor bank and the DFIG dc link of WTG *i* can be determined by

$$P_{essi,\max} = \pm C_{ess} V_{essi} \left| \frac{dV_{essi}}{dt} \right|_{\max} \qquad (17)$$
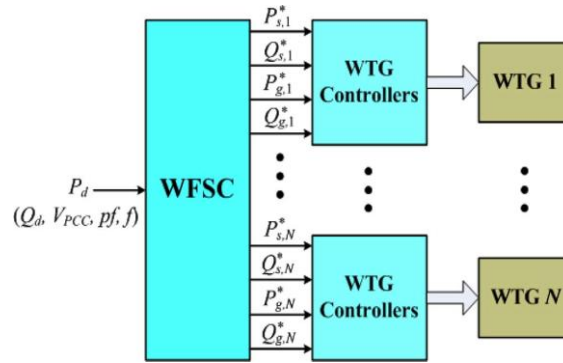

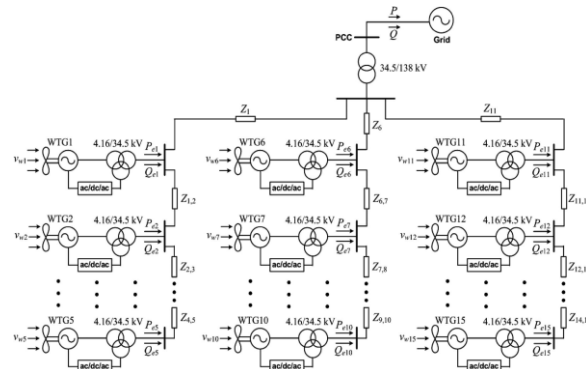**Fig. 8. Proposed two-layer CPC scheme for the wind farm.**

Fig. 9. Configuration of a wind farm equipped with 15 DFIG wind turbines connected to a power grid.

V. SIMULATION RESULTS

Simulation studies are carried out for a wind farm with 15 DFIG wind turbines (see Fig. 9) to verify the effectiveness of the proposed control scheme under various operating conditions. Each DFIG wind turbine (see Fig. 1) has a 3.6-MW power capacity [14], [15]. The total power capacity of the wind farm is 54 MW. Each DFIG wind turbine is connected to the internal network of the wind farm through a 4.16/34.5-kV voltage step-up transformer. The high-voltage terminals of all transformers in the wind farm are connected by 34.5-kV power cables to form the internal network of the wind farm. The entire wind farm is connected to the utility power grid through a 34.5/138-kV voltage step-up transformer at PCC to supply active and reactive powers of P and Q, respectively. In this paper, the power grid is represented by an infinite source. The ESS of each WTG is designed to continuously supply/store 20% of the DFIG rated power for approximately 60 s. Then, the total capacitance of the supercapacitor bank can be obtained from (1). The parameters of the WTG, the ESS, and the power network are listed in the in the Appendix. Some typical results are shown and discussed in this section.

A. CPC During Variable Wind Speed Conditions

Fig. 10 shows the wind speed profiles of WTG1 ($vw1$), WTG6 ($vw6$), and WTG11 ($vw11$). The wind speeds across the three WTGs vary in a range of ±3 m/s around their mean value of 12 m/s. The variations of wind speed cause fluctuations of the electrical quantities of the WTGs. As shown in Fig. 11, if the wind farm is not equipped with any energy storage devices or the proposed CPC scheme, the wind speed variations in the wind farm result in significant fluctuations of the total output active power at the PCC. The wind farm power output deviates significantly from the active power demand or commitment. In future electric power grids where the penetration of wind power is high (e.g., 20%), such active power fluctuations can bring severe problems to grid operation.
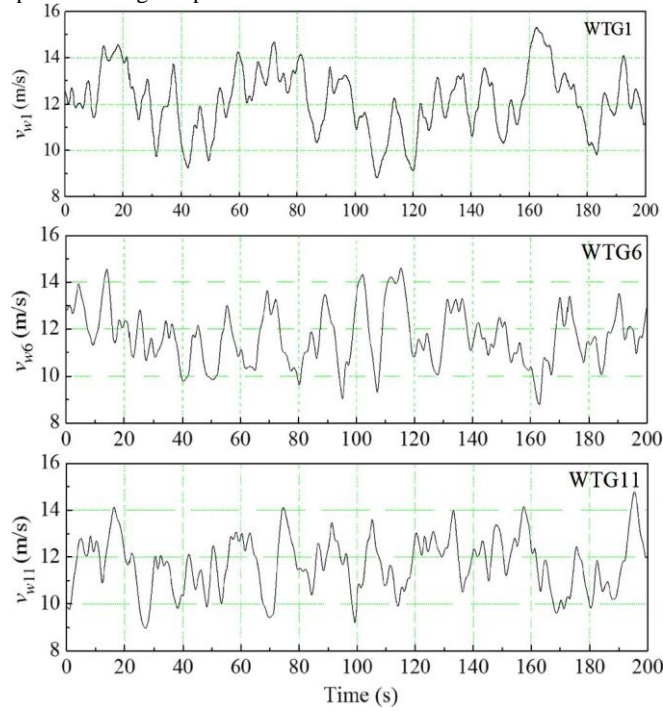

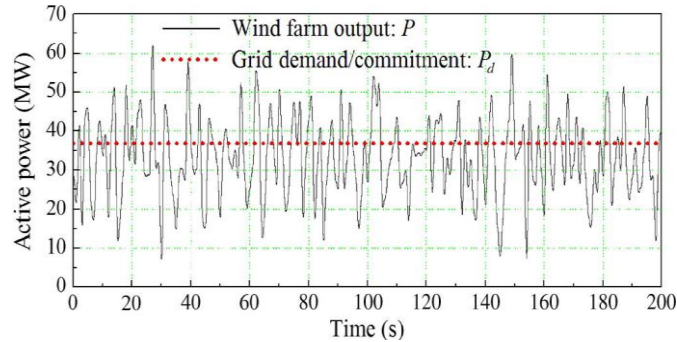*Fig. 10. Wind speed profiles of WTG1, WTG6, and WTG11.*

Fig. 11. Comparison of the wind farm power output and the constant power demand from or commitment to the grid operator: Without ESSs and the proposed CPC scheme.
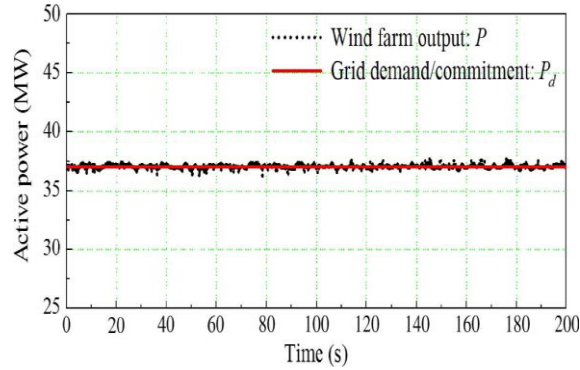
Fig. 12. Comparison of the wind farm power output

(measured at PCC) andthe constant power demand from
or commitment to the grid operator: WithESSs and the
proposed CPC scheme.

Fig. 12 compares the total output active power of the wind farm with the power demand from or commitment to the grid operator, where each WTG is equipped with an ESS as shown in Fig. 1. The ESS stores energy when the WTG generates more active power than the demand/commitment and supplies energy when the WTG generates less active power than the demand/commitment. The resulting output power of the wind farm is therefore controlled at a constant value as required by the grid operator.
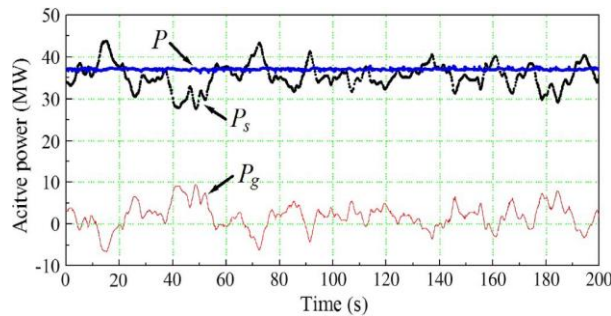

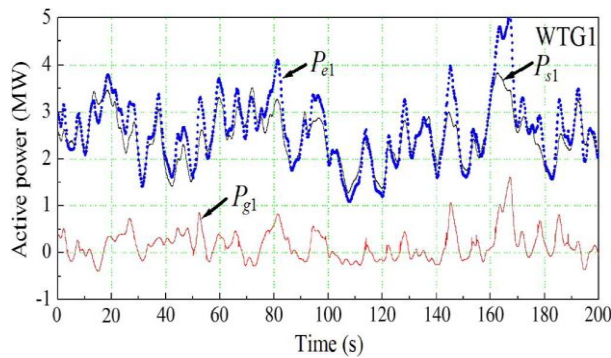**Fig. 13. Active powers of all WTGs and the wind farm.**

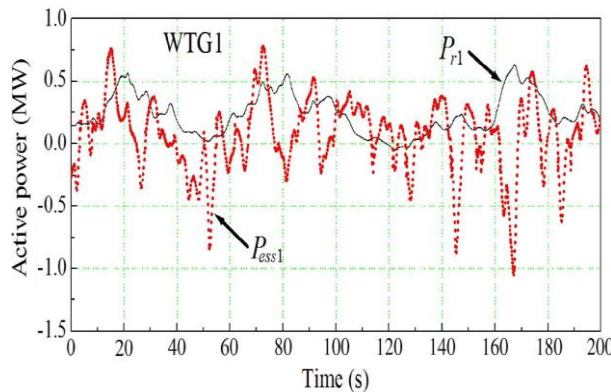**Fig. 14. Stator active power (Ps1), GSC active power (Pg1), and total active power output (Pe1) of WTG1.**

Fig. 15. Rotor active power (Pr1) and active power stored in or supplied bythe ESS (Pess1) of WTG1.

Fig. 13 shows the total stator active power *Ps* and the total GSC active power *Pg* of all WTGs, as well as the total output active power *P* (measured at PCC) of the wind farm. Through the control of the proposed CPC scheme, the variations of the stator active power are exactly compensated by the variations of the GSC active power. Consequently, the total output active power of the wind farm is constant. However, the total output active power *Pei* of each individual WTG, which is the sum of the stator active power *Psi* and the GSC active power *Pgi*, is usually not constant, as shown in Fig. 14 for WTG 1. The deviations between the RSC active power (*Pri*) and the GSC active power (*Pgi*) of each WTG are stored in or supplied by the ESS (*Pessi*), as shown in Fig. 15 for WTG 1.
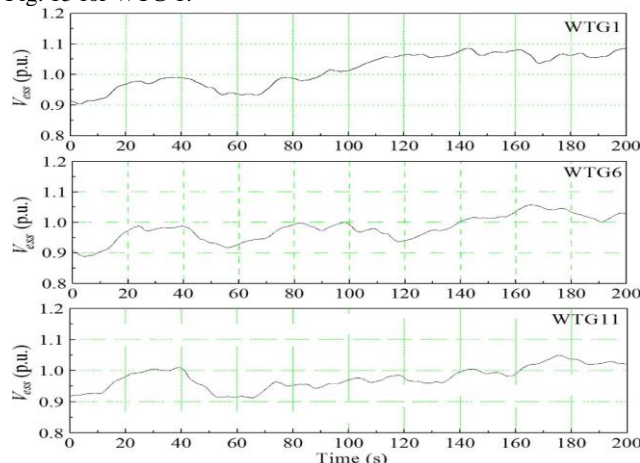

Fig. 16. Voltages of the supercapacitor banks of WTG1,WTG6, andWTG11

VI.   CONCLUSION

This paper has proposed a novel two-layer CPC scheme for a wind farm equipped with DFIG wind turbines. Each wind turbine is equipped with a supercapacitor-based ESS, which isconnected to the dc link of the DFIG through a two-quadrant dc/dc converter. The ESS serves as either a source or a sink of active power to control the generated active power of the DFIG wind turbine. Each individual DFIG wind turbine and its ESS are controlled by low-layer WTG controllers, which are coordinated by a high-layer WFSC to generate constant active power as required by or committed to the grid operator. Simulation studies have been carried out for a wind farm equipped with 15 DFIG wind turbines to verify the effectiveness of the proposed CPC scheme. Results have shown that the proposed CPC scheme enabled the wind farm to effectively participate in unit commitment and active power and frequency regulations of the grid. The proposed system and control scheme provides a solution to help achieve high levels of penetration of wind power into electric power grids.

REFERENCES

1. "Focus on 2030: EWEA aims for 22% of Europe's electricity by 2030," *Wind Directions*, pp. 25–34, Nov./Dec. 2006.
2. 20% Wind Energy By 2030: Increasing Wind Energy's Contribution to U.S. Electricity Supply, U.S. Department of Energy, Jul. 2008.
3. W. Qiao and R. G. Harley, "Grid connection requirements and solutions for DFIG wind turbines," in *Proc. IEEE Energy Conf.*, Atlanta, GA, Nov. 17–18, 2008, pp. 1–8.
4. Wind Generation & Total Load in the BPA Balancing Authority: DOE Bonneville Power Administration, U.S. Department of Energy. [Online]. Available:
5. R. Piwko, D. Osborn, R. Gramlich, G. Jordan, D. Hawkins, and K. Porter, "Wind energy delivery issues: Transmission planning and competitive electricity market operation," *IEEE Power Energy Mag.*, vol. 3, no. 6, pp. 47–56, Nov./Dec. 2005.
6. L. Landberg, G. Giebel, H. A. Nielsen, T. Nielsen, and H. Madsen, "Shortterm prediction—An overview," *Wind Energy*, vol. 6, no. 3, pp. 273–280, Jul./Sep. 2003.
7. M. Milligan, B. Kirby, R. Gramlich, and M. Goggin, Impact of Electric Industry Structure on High Wind Peneration Potential, Nat. Renewable Energy Lab., Golden, CO, Tech. Rep. NREL/TP-550-46273. [Online]. Available: http://www.nrel.gov/docs/fy09osti/46273.pdf
8. J. P. Barton and D. G. Infield, "Energy storage and its use with intermittent renewable energy," *IEEE Trans. Energy Convers.*, vol. 19, no. 2, pp. 441– 448, Jun. 2004.
9. D. Rastler, "Electric energy storage, an essential asset to the electric enterprise: Barriers and RD&D needs," *California Energy Commission Staff Workshop Energy Storage Technol., Policies Needed Support California's RPS Goals 2020*, Sacramento, CA, Apr. 2, 2009.
10. C. Abbey and G. Joos, "Supercapacitor energy storage for wind energy applications," *IEEE Trans. Ind. Appl.*, vol. 43, no. 3, pp. 769–776, May/Jun. 2007.
11. B. S. Borowy and Z. M. Salameh, "Dynamic response of a stand-alone wind energy conversion system with battery energy storage to wind gust," *IEEE Trans. Energy Convers.*, vol. 12, no. 1, pp. 73 78, Mar. 1997.
12. M.-S. Lu, C.-L. Chang, W.-J. Lee, and L. Wang, "Combining the wind power generation system with energy storage equipments," *IEEE Trans. Ind. Appl.*, vol. 45, no. 6, pp. 2109–2115, Nov./Dec. 2009.